Cell Communication and Signaling

RESEARCH

Open Access

GZMA suppressed GPX4-mediated ferroptosis to improve intestinal mucosal barrier function in inflammatory bowel disease

Rongwei Niu[1,2†], Jiaoli Lan[3,4†], Danxia Liang[5], Li Xiang[2], Jiaxin Wu[3], Xiaoyan Zhang[3], Zhiling Li[3], Huan Chen[2], Lanlan Geng[2], Wanfu Xu[2*], Sitang Gong[1,2*] and Min Yang[3,5*]

Abstract

Background Our previous study has demonstrated a decreased colonic $CD8^+CD39^+$ T cells, enrichment of granzyme A (GZMA), was found in pediatric-onset colitis and inflammatory bowel disease (IBD) characterized by impaired intestinal barrier function. However, the influence of GZMA on intestinal barrier function remains unknown.

Methods Western blotting(WB), real-time PCR (qPCR), immunofluorescence (IF) and in vitro permeability assay combined with intestinal organoid culture were used to detect the effect of GZMA on intestinal epithelial barrier function in vivo and in vitro. Luciferase, immunoprecipitation (IP) and subcellular fractionation isolation were performed to identify the mechanism through which GZMA modulated intestinal epithelial barrier function.

Results Herein, we, for the first time, demonstrated that $CD8^+CD39^+$ T cells promoted intestinal epithelial barrier function through GZMA, leading to induce Occludin(OCLN) and Zonula Occludens-1(ZO-1) expression, which was attributed to enhanced CDX2-mediated cell differentiation caused by increased glutathione peroxidase 4(GPX4)-induced ferroptosis inhibition in vivo and in vitro. Mechanically, GZMA inhibited intestinal epithelial cellular PDE4B activation to trigger cAMP/PKA/CREB cascade signaling to increase CREB nuclear translocation, initiating GPX4 transactivity. In addition, endogenous PKA interacted with CREB, and this interaction was enhanced in response to GZMA. Most importantly, administration of GZMA could alleviate DSS-induced colitis in vivo.

Conclusion These findings extended the novel insight of GZMA contributed to intestinal epithelial cell differentiation to improve barrier function, and enhacement of GZMA could be a promising strategy to patients with IBD.

Keywords GZMA, Ferroptosis, CDX2, Intestinal barrier function, IBD

†Rongwei Niu and Jiaoli Lan contributed equally to this work.

*Correspondence:
Wanfu Xu
xuwanfu@gzhmu.edu.cn
Sitang Gong
gongsitang@hotmail.com
Min Yang
ymlyxw@hotmail.com
[1]The First Affiliated Hospital of Jinan University, Jinan University, Guangzhou, China
[2]Department of Gastroenterology, Guangzhou Women and Children's Medical Center, Guangzhou Medical University, Guangzhou 510623, China
[3]Department of Pediatrics, Guangdong Provincial People's Hospital, Guangdong Academy of Medical Sciences, Southern Medical University, Guangzhou 510080, China
[4]Research Center of Medical Sciences, Guangdong Provincial People's Hospital, Guangdong Academy of Medical Sciences, Guangzhou, China
[5]School of Medicine, South China University of Technology, Guangzhou 510006, China

Background

Inflammatory bowel disease (IBD) is a chronic, relapsing inflammatory disorder of the gastrointestinal tract, including Ulcerative colitis (UC) and Crohn's disease (CD), which is characterized by dysregulation of intestinal barrier function [1–3]. The interaction between OCLN and ZO-1 has been showed to play a crucial role in the formation of tight junctions in IECs [4], serving as a critical barrier to effectively prevent the infiltration of harmful bacteria and toxins from the intestines into the body. Interestingly, a series of studies has revealed GPX4 and solute carrier family 7 member 1(SLC7A11; also called xCT)-mediated ferroptosis inhibition, an iron-dependent form of cell death, could promote CDX2 expression [5], which further enhanced ZO-1 and OCLN expression, thereby maintaining intestinal barrier function [6–9]. However, the specific mechanisms through which regulates ferroptosis in IBD remained unclear.

Numerous studies have found that the occurrence of IBD is associated with excessive ferroptosis activation in the intestine. For instance, ferroptosis was prominently triggered by various signaling pathways, including endoplasmic reticulum stress signaling in IECs of both UC patients and DSS-induced colitis [10], while impaired GPX4 activity and signs of lipid peroxidation were observed in CD [11]. Interestingly, the work from Pan et al. showed that PDE4/cAMP/PKA/CREB cascade signaling is critical for GPX4 expression in intestinal epithelial cells [12], and inhibition of PDE4 could enrich intestinal mucosal $CD8^+CD39^+$T cells, improving the intestinal inflammation and barrier function in IBD [13]. However, the possible role of intestinal mucosal $CD8^+CD39^+$T cells in improvement of intestinal barrier function has not been addressed yet.

Of note, our previous research has revealed an enrichement of GZMA levels in $CD8^+CD39^+$T cells [13]. Currently, the function of GZMA is largely focused on cancer and cell death. GZMA, a serine protease secreted by cytotoxic T lymphocytes (CTLs) and natural killer (NK) cells, could induce IL-6 production in macrophages, which in turn activates STAT3 phosphorylation to promote the development of colorectal cancer [14, 15]. In addition, the killer lymphocyte protease GZMA can promote cell pyroptosis through perforin and trigger caspase-independent target cell death with morphological features of apoptosis [16, 17]. CTLs induce apoptosis through the engagement of death receptors or the exocytosis of cytolytic granules containing granzyme proteases and perforin [18]. Herein, we further demonstrated the novel role of GZMA in IBD that GZMA could promote intestinal epithelial barrier function, and established an unreported mechanism of GZMA promoted intestinal barrier function through GPX4-mediated ferroptosis.

Methods and materials

Reagents and antibodies

Recombinant Human GZMA (YA9870) was purchased from atagenix (Wuhan, China); RSL3 (HY-100218 A), Rp-cAMPS (HY-100530D), Dipyridamole (HY-B0312) and FITC-Dextran(HY-128868 A) were purchased from MedChemExpress (Shanghai, China); GPX4-shRNA plasmid, CREB1-shRNA plasmid, CDX2 promoter plasmid and GPX4 promoter plasmid were purchased from Youbio (Changsha, China); Lipofectamine 8000(C0533) was purchased from Beyotime(Shanghai, China); Antibodies targeting CD8α(ab251596, 1:1000 for IF), CD39(ab300065, 1:250 for IF), Human Granzyme A ELISA Kit (ab255728) and cAMP ELISA Kit(ab138880) were purchased from Abcam (UK). Antibodies targeting GPX4(67763-1-Ig, 1:400 for IF, 1:2000 for WB), SLC7A11(26864-1-AP, 1:200 for IF, 1:2000 for WB), CDX2(60243-1-Ig, 1:2000 for WB), CREB1(12208-1-AP, 1:200 for IF, 1:2000 for WB), PRKACA(27398-1-AP, 1:2000 for WB), ZO-1(21773-1-AP, 1:1000 for IF, 1:5000 for WB), Occludin(13409-1-AP, 1:1000 for IF, 1:2000 for WB), GAPDH(10494-1-AP, 1:5000 for WB), Granzyme A (11288-1-AP, 1:200 for IF) were from Proteintech Company (Wuhan, China); PRKACA(ER1706-65, 1:200 for IF), EpCAM(EM1111, 1:200 for IF) was purchased from HUABIO (Hangzhou, China); a-tublin(RM2007, 1:5000 for WB), b-actin(RM2001, 1:5000 for WB) were purchased from Ray antibody biotech (Beijing, China); Phospho-CREB1(Ser133) (YP0075, 1:2000 for WB), PDE4 (YP0668, 1:1000 for WB), Phospho-PDE4(Ser133/119/190) (YP0668, 1:2000 for WB, 1:200 for IF) were from Immunoway Research (Plano, USA); Phospho-PKA C (Thr197) (4781, 1:1000 for WB) was from Cell Signaling Technology (Danvers, USA); Lamin A/C (sc-376248, 1:3000 for WB) was from Santa Cruz Biotechnology (Dallas, Texas, USA); PE anti-human CD3 (300408, clone UCHT1), FITC anti-human CD4 (317407, clone OKT4), PerCP/Cyanine5.5 anti-human CD8α (300923, clone HIT8a) and APC anti-human CD39 (328209, clone A1) were from Biolegend (San Diego, USA). CDX2 monoclonal antibody(14H6) (YM3057, 1:200 for IF), Alexa-488- and 594-conjugated secondary antibodies were from Immunoway (Beijing, China).

Cell culture and transfection

Caco-2, HT-29 and HEK293T cells were purchased from the American Type Culture Collection (ATCC, Manassas, USA) and cultured in DMEM (Dulbecco's Modified Eagle Medium) supplemented with 10% Fetal Bovine Serum (FBS), 100 mg/ml streptomycin and 100 U/ml penicillin. Cells were maintained in a carbon dioxide (CO2) incubator set to a standard culture condition of 37 °C and 5% CO2. The plasmids were delivered into cells with lipofectamine 8000 according to manufacturer's instruction.

Enzyme-linked immunosorbent assay (ELISA)

Peripheral blood, human colon tissues, mouse colon tissues, Caco-2 cell lysates were collected. Human GZMA level in Peripheral blood and human colon tissues, and cAMP content in mouse colon tissues and cell lysates were measured using corresponding elisa kit according to the manufacturer's instructions.

RNA extraction and quantitative real-time PCR

Total RNA was isolated from Caco-2 and HT-29 cells, as well as from mouse colon tissues, using the EZ-press RNA Purification Kit (B0004D). Reverse transcripted into cDNA was performed using PrimeScript™ RT Master Mix (TAKARA, Japan). Quantitative PCR (qPCR) was carried out using the TB Green Premix Ex Taq ™ II (TAKARA, Japan) according to the manufacturer's instructions. The Primer sequence used in this study are listed in supplementary Table 1.

Western blotting (WB) analysis

For protein extraction, Caco-2 and HT-29 cells were lysed using a RIPA lysis buffer (Biosharp, China) containing protease inhibitors and quantified by the BCA kit. Nuclear and cytosolic proteins were separated by nuclear extraction kit (Beyotime, China). equal amounts of protein samples were loaded onto SDS-PAGE gels and subjected to electrophoresis. The proteins were then transferred onto a nitrocellulose membrane, which was further blocked to prevent non-specific binding. Next, addition of the primary antibodies to incubate indicated band overnight at 4 °C, subsequently, the further incubation with secondary antibodies was performed after washing. the protein bands were visualized using a chemiluminescent substrate (Perkin Elmer).

ROS detection

The intracellular ROS level was analyzed using the Reactive Oxygen Species Assay Kit (BL714A, Biosharp, Anhui, China) according to the manufacturer's instruction.

In vitro permeability assay

As described previously [19], a total of 1×10^5 Caco-2 cells were seeded onto 0.4 μm porous Transwell polycarbonate membranes (Transwell 3401; Corning, NY, USA) pre-inserted in 12-well plates. Subsequently, the cells were cultured and media was refreshed every two days. After confluence (18–21 days after seeding), cells were exposed to GZMA (500 nM) or RSL3(5 μM) for 48 h. 1 mg/mL fluorescein isothiocyanate (FITC)-dextran (4 kDa) was added to insert to incubate for 2 h at 37 °C. The permeability of the monolayer to FITC-dextran was assessed by quantifying the fluorescence intensity in the lower chamber using an excitation wavelength of 485 nm and an emission wavelength of 535 nm. The fluorescence values were converted into FITC-dextran concentrations (pg/mL) using a standard curve. A total of three independent experiments were conducted.

Luciferase reporter assay

HEK293T cells were co-transfected with the Luc-GPX4 or Luc-CDX2 promoter plasmid and internal control plasmid (pGL4.74) using Lipofectamine 8000 according to manufacturer's instruction. After 24 h of transfection, GZMA (500 nM) was added into the cells to incubate for another 24 h. The RLU were measured using Duo-Lite Luciferase Assay System (Nanjing, China).

Immunofluorescence (IF) analysis

HT-29 and Caco-2 cells were digested and reseeded at a density of $0.5*10^5$/mL in 6-well plates overnight. After GZMA treatment, cells were fixed in 4% paraformaldehyde for 15 min, washed three times with PBS for 5 minutes and then blocked in 10% goat serum for 1 h. Cells were incubated with the primary antibodies overnight at 4 °C. For the tissue slides, after deparaffinization, the blocking solution (PBS with 5% normal donkey or goat serum and 0.3% Triton X-100) was used to incubate for 30 min at room temperature. The further incubation was performed with the primary antibody overnight at 4 °C. The next day, secondary antibody was used to incubate for 1 h at room temperature after washing. The coverslips were mounted onto glass slides with prolong gold reagent after staining the nuclei with 4′,6-diamidino-2-phenylindole (DAPI). Stained cells were visualized using a laser scanning fluorescent microscope.

Immunoprecipitation

After treatment with GZMA (500 nM) or DIP (5 μM) for 1 h, HT-29 or Caco-2 cells were lysed in RIPA for 15 min and incubated with antibodies targeted PKA or IgG at 4 °C overnight. The next day, Protein A/G beads (LSKMAGAG10, Millpore) was added into the lysate mixture to incubate another 2 h. The lysate was centrifugated to remove the supernatant, the mixture was lysated with loading buffer and analyzed by western blots.

Flow cytometry

PBMCs from healthy donors were isolated by Ficoll density gradient. For surface staining, single-cell suspensions were incubated with FACS antibodies in FACS buffer, which consisted of PBS with 2% BSA and 5 mM EDTA, for 20 min at 4 °C. The antibodies used for staining included PE anti-human CD3 (300408, clone UCHT1), FITC anti-human CD4 (317407, clone OKT4), PerCP/Cyanine5.5 anti-human CD8a (300923, clone HIT8a), APC anti-human CD39 (328209, clone A1). Flow cytometry was performed using a cytometer (FACSAria fusion,

BD) and the acquired data were analyzed using FlowJo v.10.0.7 software.

Crypt isolation, culture, and the generation of organoids

As described in our previous work [5], euthanizing the mice according to ethical regulations, the intestinal tissues were aseptically harvested. The surrounding mesentery and adipose tissues were removed by washing the intestines with cold DPBS. The intestinal tissues were then cut into 2 mm-wide sections and digested using Gentle Cell Dissociation Reagent cGMP (STEMCELL, 100–0485) on a shaker with a speed of 300 rpm at 4 °C to release crypts. The tissue suspension was filtered through a 70 μm filter, and the collected tissue suspension passed through the filter and suspended with intestiCult™ Organoid Growth Medium (Mouse, STEMCELL, 06005) for culture. GZMA (500 nM) and RSL3 (5 μM) were added to observe the effect on intestinal organoids generation.

DSS-induced chronic colitis model

As described in our previous study [20], mice aged 6–8 weeks were induced by 2% (w/v) dextran sulfate sodium (DSS, Millipore Corporation, Billerica, MA, USA) in drinking water for 7 days, and followed by GZMA, RSL3 or vehicle treatment. GZMA was administered via intraperitoneal injection at a dose of 20 μg per mouse on day 0, day 2, day 4, and day 6. RSL3 was administered at a dose of 10 mg/kg via intraperitoneal injection on the same days. The body weight changes and overall survival were recorded daily. On day 7, mice were scarified, and the colon was isolated for pathological analysis.

Histopathology

The intestinal samples were initially fixed in 10% formalin, followed by embedding in paraffin and slicing into 4 μm thick sections for histopathological examination. Hematoxylin and eosin (H&E) staining was performed to visualize tissue structures and identify pathological changes. Slides were observed using a light microscope (DMI8, Leica), and images were captured for further analysis. The histopathological score for each section was referenced to previous studies. The criteria are listed in supplementary Table 2.

Statistical analysis

Statistical analyses were performed with GraphPad Prism 9.0. Unless otherwise stated, data were presented as mean ± SD. P value < 0.05 was taken to indicate statistical significance.

Results

GZMA was decreased in patients with IBD and DSS-induced colitis

To explore the change of GZMA expression in IBD, We firstly utilized ELISA to assess the concentration of GZMA in the serum and colonic tissues of patients with IBD. The results showed that a significant downregulation of GZMA levels was observed in compared to healthy controls in both the serum and colonic tissues of IBD patients. (Fig. 1A-B). In line with this, the GZMA mRNA level in the colon of DSS-treated mice was largely decreased compared to that in normal mice, indicative of a significant increase in IL-6 expression, a marker of intestinal inflammation(Fig. 1C). In addition, immunofluorescence analysis further confirmed GZMA expression in $CD8^+CD39^+$ T cells was reduced in the intestinal mucosa of IBD patients (Fig. 1D).

GZMA induced intestinal epithelial cell differentiation

Previous studies have implied GZMA might have a role in cell differentiation due to the work showed that GZMA depletion led to a significant osteoclast differentiation [21, 22], which focused us to explore the possible effect of GZMA on intestinal epithelial cell differentiation. As shown in Fig. 2A, CDX2, a mastor of intestinal epithelial cell differentiation, was found to be significantly reduced in the intestinal mucosa, which focused us to explore the possible role of $CD8^+CD39^+$ T cells-derived GZMA on CDX2 expression. Next, the 21-day Caco-2 monolayer transwell system [19, 23–25] was employed to assess the effect of GZMA on intestinal epithelial cell integrity (Fig. 2B). As expected, a significant downregulation of trans-epithelial flux of FITC-dextran in polarized Caco-2 cells was observed after GZMA treatment (Fig. 2C), which was attributed to enanced intestinal epithelial cell differentiation as evidenced by increased CDX2, ZO-1 and OCLN mRNA and protein level(Fig. 2D-F). In line with this, immunofluorescence analysis also confirmed that GZMA upregulated ZO-1 and OCLN expression in Caco-2 (Fig. 2G).

Interestingly, GZMA treatment could increase the budding of intestinal organoids (Fig. 2H), and depletion of CDX2 expression in Caco-2 could reverse the effect of GZMA on ZO-1 and OCLN expression, indicating that GZMA modulated intestinal epithelial integrity through enhancing CDX2 expression (Fig. 2I). most importantly, addition of anti-GZMA in co-cultured system could rescue the influence of $CD8^+CD39^+$ T cells isolated from PBMCs from healthy donors' peripheral blood on CDX2, ZO-1 and OCLN expression (Fig.S1F, Fig. 2J-K). Taken together, these data suggested that GZMA is critical mediator in $CD8^+CD39^+$ T cells-maintained intestinal epithelial barrier function through CDX2.

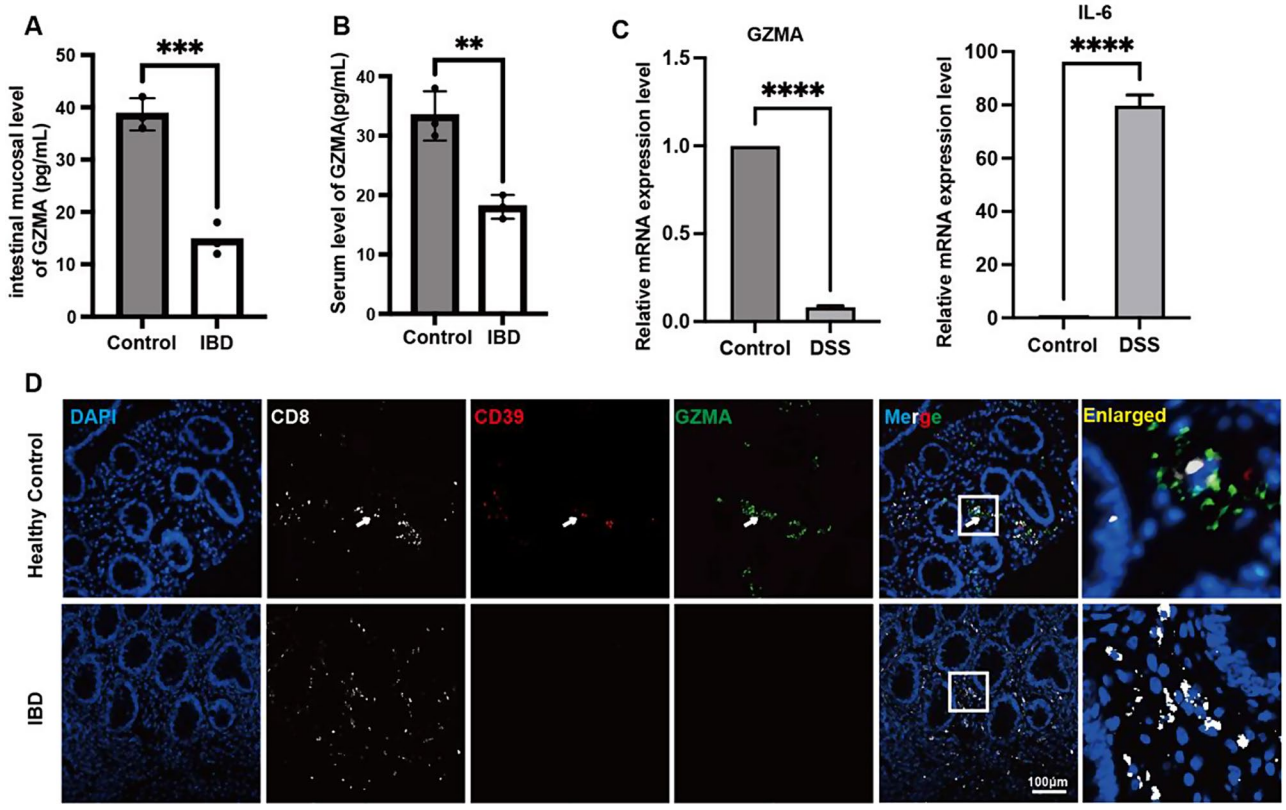

Fig. 1 Decreased GZMA in patients with IBD and DSS-induced colitis. (**A**-**B**) The level of GZMA in serum and colonic mucosa were measured by ELISA according to the instruction. Data was displayed as the means ± s.d. of three independent experiments and analyzed by two-sample t test for significance, ***$p < 0.001$, **$p < 0.01$. **(C)** Real-time PCR was employed to assess colonic GZMA and IL-6 mRNA level in indicated group. Data was exhibited as the means ± s.d. of three independent experiments and analyzed by one-sample t-test for significance, ****$p < 0.0001$. **(D)** Immunofluorescence assay was performed to detect CD8, CD39, and GZMA expression in indicated group (Scale bar: 100 μm)

GZMA promoted CDX2 expression through ferroptosis inhibition

Next, we sought to ask how GZMA regulated CDX2 expression. Previous studies have found that ferroptosis is prominently triggered in IECs of both UC patients and DSS-induced colitis [10], which attracted us to study the relationship between CDX2 and ferroptosis. A time course of Caco-2 cells differentiation showed that GPX4 expression was gradually enhanced during intestinal epithelial cells differentiation characterized by increased CDX2 expression, despite no significant difference in SLC7A11 expression was observed (Fig. 3A). Further results revealed that $CD8^+CD39^+$ T cells-derived GZMA or GZMA alone could inhibit ferroptosis characterized by enhanced GPX4 and SLC7A11 mRNA and protein levels as well as reduced ROS level (Fig. 3B-E). Moreover, immunoblotting, intestinal organiods, the trans-epithelial assessment and luciferase assay showed that activation of ferroptosis by RSL3 could reverse the promotion of GZMA on CDX2-dependent ZO-1 and OCLN expression (Fig. 3F-H, Fig.S2A-2C). what's more, the similar phenomenon was observed in IECs treated with GZMA after specific GPX4 slienced by shRNA plasmids (Fig.S2D).

To provide insights into the effect of GZMA and RSL3 in vivo, DSS-induced colitis model was employed to confirm the in vitro results combined with intraperitoneal injection of 20 ug GZMA or RSL3 at a dose of 10 mg/kg on days 0, 2, 4, and 6. As shown in Fig. 2I-L, GZMA-treated mice were shown to be protected from experimental colitis, as evidenced by enhanced mean bodyweight and colon length as well as alleviation of intestinal inflammation, while RSL3 administration displayed an impaired effect against GZMA, including CDX2, ZO-1 and OCLN expression detected by IF analysis. In summary, these work suggested GZMA induced CDX2-mediated IECs differentiation to improve epithelial integrity through inhibition of GPX4-mediated ferroptosis.

GZMA-mediated ferroptosis required CREB

It has been demonstrated that CREB plays a role in the transactivation of GPX4 [26]. Therefore, we intended to investigate whether CREB is required in the regulation of GZMA-mediated GPX4 expression in IECs.

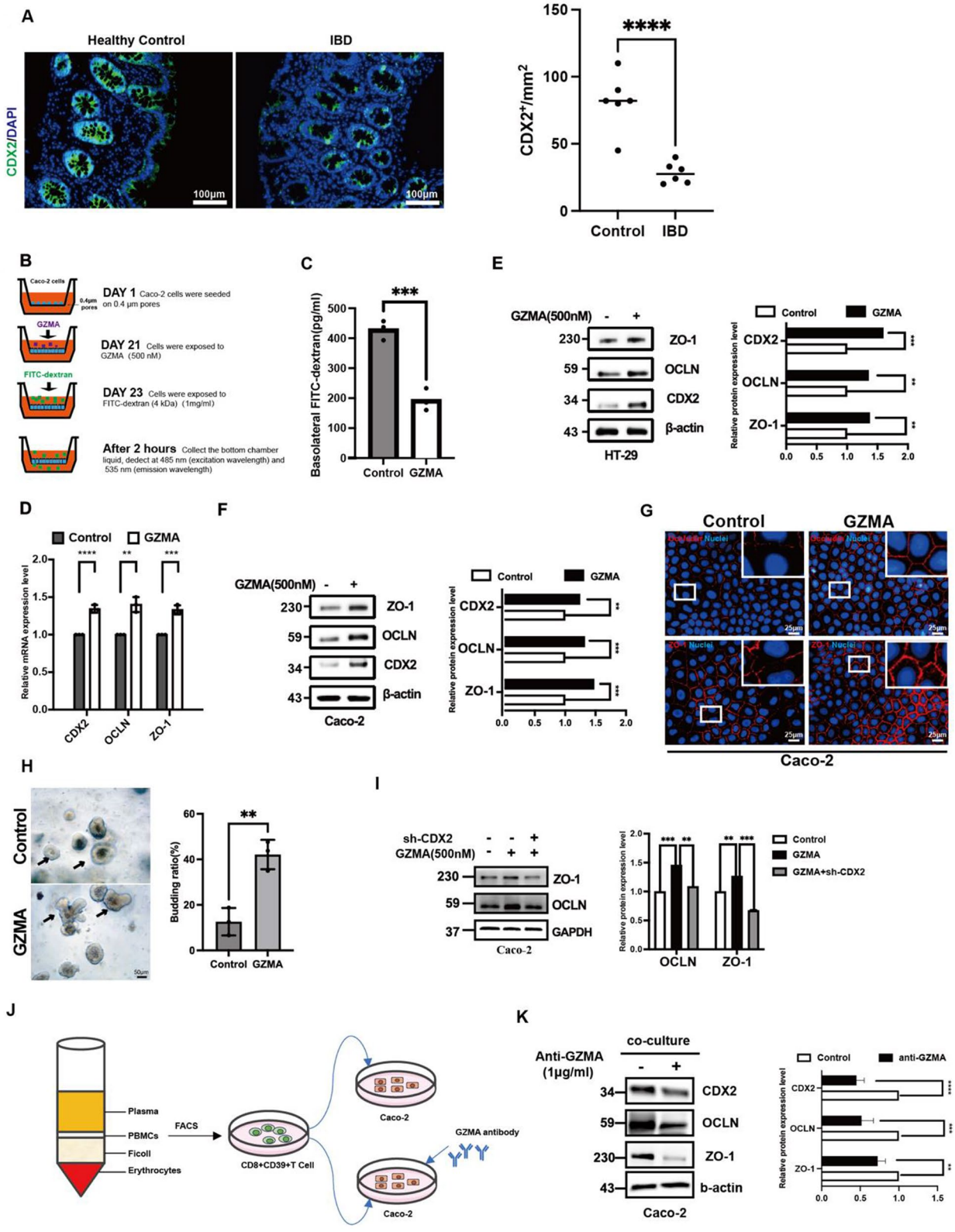

Fig. 2 (See legend on next page.)

(See figure on previous page.)

Fig. 2 GZMA promoted intestinal epithelial cell differentiation. (**A**) Immunofluorescence assay was performed to detect CDX2 expression of colonic mucosa from clinical sample (Scale bar: 100 μm), quantitation was performed by Image J, and analyzed by two-sample t test, ∗∗∗$p < 0{:}001$. **(B-C)** Caco-2 cells were seeded onto transwell polycarbonate membranes (0.4 μm pores). Upon confluence (21 days after seeding), the cells were treated with GZMA (500 nM) for up to 48 h. The permeability of the monolayer to FITC-dextran (4 kDa) was assessed by measuring the fluorescence intensity in the bottom chamber at Ex/Em = 485/535 nm. Data was displayed as means ± s.d. of three independent experiments and analyzed by two-sample t test for significance, ***$p < 0.001$.**(D)** Real-time PCR and **(E-F)** western blotting as well as **(G)** immunofluorescence staining were conducted to analyze the indicated gene expression at mRNA and protein level in HT-29 and Caco-2 cells treated with or without GZMA (500 nM) for 48 h (Scale bar: 25 μm), Data was showed as the means ± s.d. of three independent experiments and quantified by one-sample t test for significance, ***$p < 0.001$, **$p < 0.01$, *$p < 0.05$. **(H)** intestinal crypt isolated from mice was used to explore the effect of GZMA (500 nM) on intestinal organoid generation, microscopic examination of organoids was employed to calculate the proportion of budding organoids among every average 100 organoids. Data was exhibited as means ± s.d. of three independent experiments and analyzed by two sample t test, **$p < 0.01$ (Scale bar: 50 μm). **(I)** western blotting was conducted to analyze the indicated proteins in Caco-2 cells after transferred with sh-CDX2 plasmid, followed by stimulation with GZMA (500 nM) for 48 h, with β-actin serving as the internal control. **(J-K)** $CD8^+CD39^+$ T cell subsets isolated from peripheral blood of healthy donors were cultured in medium for 24 h was collected to co-culture with Caco-2 cells for 48 h combined with or without GZMA antibody supplementation. The total lysate was harvested to detect indicated proteins, Data was displayed as mean ± s.d. of three independent experiments and analyzed by one-sample t test for significance, ***$p < 0.001$, **$p < 0.01$

Subcellular fraction isolation and immunofluorescence were performed to detect the nuclear localization of CREB in response to GZMA stimulation. As shown in Fig. 4A-B, nuclear CREB level and nuclear translocation was drastically increased in HT-29 and Caco-2 cells after GZMA treatment. What's more, inhibition of CREB largely reversed the effect of GZMA on GPX4, CDX2, and downstream proteins (Fig. 4C, Fig.S3A). Furthermore, we found that the GPX4 transactivation induced by GZMA was reversed after CREB depleted in HEK293 cells (Fig. 4D). Altogether, these results suggested GZMA promoted GPX4 expression through CREB.

GZMA triggered PDE4/PKA/CREB cascade signaling

The above results indicated that CREB is crucial for GZMA-mediated ferroptosis in IECs, highlighting its significance. PKA phosphorylated CREB to enhance CREB nuclear translocation to initiate target genes expression [27]. Therefore, we tried to investigate the impact of the cAMP/PKA/CREB cascade signaling in response to GZMA due to the previous work from our lab demonstrated that this pathway was critical for GPX4 expression [12]. As shown in Fig. 5A, cAMP level was increased in colon tissue from DSS group after GZMA administration in vivo, and in vitro also confirmed GZMA could induce cAMP gerentiation. What's more, addition of Rp-cAMPS, a PKA inhibitor, largely blocked the effect of GZMA on ferroptosis and CDX2 as well as downstream targets expression in Caco-2 cells(Fig. 5B). Of note, further work showed that GZMA could suppress PDE4 phosphorylation, leading to increase cAMP generation in vivo and in vitro, which further triggered PKA/CREB activation, while no significant changes of AC6 was observed (Data not shown) (Fig. 5C). Most importantly, GZMA-induced endogenous PKA/CREB complex colocalization was enhanced after PDE4 inhibitor dipyridamole (DIP) (Fig. 5D-E). These results suggested that GZMA inhibited ferroptosis through activation of PDE4/PKA/CREB signaling pathway.

Ferroptosis inhibition caused by GZMA administration ameliorated DSS-induced colitis

In vitro work has demonstrated GZMA alleviated PDE4-mediated ferroptosis to promote CDX2 expression providing insights into the effect of GZMA on ferroptosis in vivo, DSS-induced colitis model combined with intraperitoneal injection of 20 μg GZMA on days 0, 2, 4, and 6 was employed to confirm the above results. As shown in Fig. 6A-B, GZMA-treated mice was exhibited to be protected from experimental colitis as evidenced by mean bodyweight and colon length. Further work showed that decreased ferroptosis, characterized by enhanced GPX4 and xCT in IECs labeled with EpcAM was observed after GZMA administration in DSS group, which was attributed to PDE4 phosphorylation inhibition confirmed by immunofluorence (Fig. 6C). Taken together, these results suggested that GZMA is critical for improvement of intestinal barrier function through modulating PDE4-mediated ferroptosis.

Discussion

In this study, as shown in Fig. 6D, our work extended the role of GZMA in IBD and presented evidence to support the promotion of GZMA on IECs differentiation. Mechanically, GZMA suppressed phosphorylation of PDE4, leading to trigger PKA/CREB cascade signaling, which further enhance CREB nuclear translocation and the binding of CREB to GPX4 promoter, subsequently induced GPX4-dependent CDX2 expression to improve intestinal barrier intergrity. What's more, ferroptosis inhibition or GPX4 depletion could overcome the effect of GZMA in IECs. Most importantly, intraperitoneal injection of GZMA could rescue the symptoms of DSS-induced colitis in vivo. These findings indicated the significant role of GZMA in regulating IECs barrier intergity through the PDE4/PKA/CREB pathway.

Currently, there are ongoing studies investigating the role of GZMA in cell death during development, tissue maintenance, immune response, elimination of excess cells, defense against pathogens, and cancer prevention

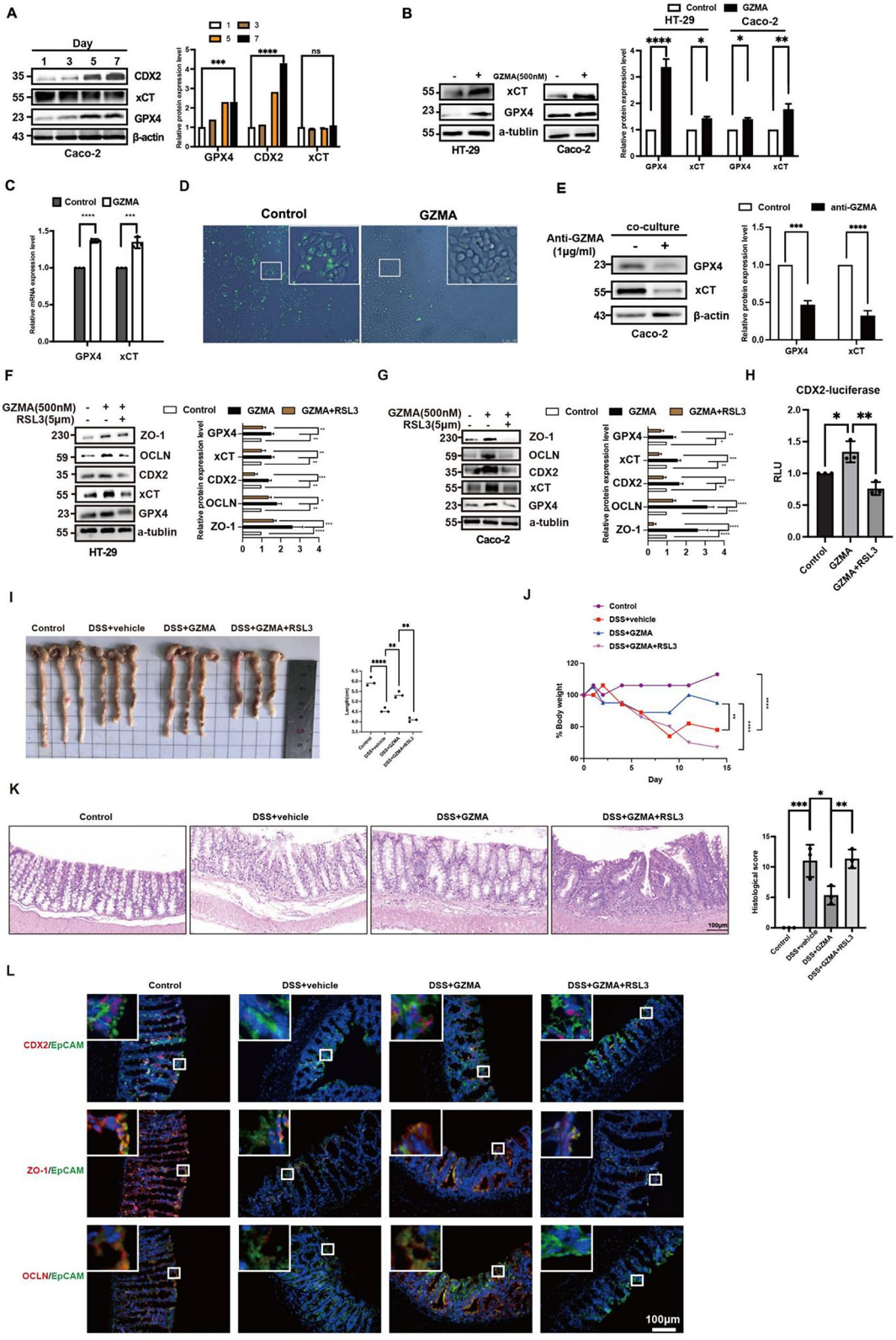

Fig. 3 (See legend on next page.)

(See figure on previous page.)

Fig. 3 GZMA promoted intestinal epithelial cell differentiation through inhibition of ferroptosis. (**A**) Lysate was extracted from Caco-2 at day 1/3/5/7 post-confluence, and the expression of target proteins were analyzed by western blotting. Data was represented the mean ± s.d. of three independent experiments and determined by one-way ANOVA for significance, $^{****}p < 0.0001$, $^{***}p < 0.001$. HT-29 and Caco-2 cells were treated with GZMA (500 nM) for 48 h, WB **(B)** and qPCR **(C)** were employed to determine indicated gene at mRNA and protein level. The control was normalized as 1. The band intensity and relative mRNA expression was represented as mean ± s.d. of three independent experiments and analyzed by one-sample t test for significance, $^{***}p < 0.001$, $^{**}p < 0.01$, $^{*}p < 0.05$. **(D)** After serum starvation for 24 h, Caco-2 cells were treated with GZMA (500 nM) for 48 h and the ROS level was detected. **(E)** immunoblotiting was performed to detect indicated protein in coculture model established by $CD39^{+}CD8^{+}$ T cell and Caco-2 cells combined with or without anti-GZMA addition, Data was displayed as the mean ± s.d. of three independent experiments and analyzed using one sample t test for significance, $^{****}p < 0.0001$, $^{***}p < 0.001$. The control was normalized to 1. **(F-G)** HT-29 and Caco-2 cells were treated with GZMA (500 nM) combined with or without RSL3 (5 μM) for 48 h, WB was conducted to analyze the indicated protein. Data was presented as the means ± s.d. of three independent experiments and analyzed by one-way ANOVA and Dunnett's multiple comparison test, $^{****}p < 0.0001$, $^{***}p < 0.001$, $^{**}p < 0.01$, $^{*}p < 0.05$. **(H)** After co-transfection with CDX2-luc plasmid and a control renilla luciferase vector for 12 h, 293T cells were treated with GZMA (500 nM) or GZMA (500 nM) combined with RSL3 (5 μM) for 48 h, the relative luciferase unit (RLU) was measured. Data was presented as the means ± s.d. of three independent experiments and analyzed by one-way ANOVA, $^{*}p < 0.05$,$^{**}p < 0.01$. **(I)** Image of colon length and **(J)** body weight change in indicated group were exhibited. the percentage of initial body weight at the start of the experiments as 100%. Statistical difference was determined by one way ANOVA analysis, $^{****}p < 0.0001$, $^{**}p < 0.01$. (**K**) HE staining of representative colon mucosa and scored to determine difference using one way ANOVA in indicated groups, $^{*}p < 0.05$,$^{**}p < 0.01$,$^{***}p < 0.001$. (**L**) Immunofluorescence was performed to detect CDX2, ZO-1, and OCLN expression in indicated group

[28]. Limited available work about the role of GZMA in IBD, despite our previous work revealed GZMA was enriched in $CD8^{+}CD39^{+}$ T cells, decreased in intestinal mucosa in IBD. In line with this work that demonstrated GZMA could promote the differentiation of IECs through ferroptosis, an observational study on UC received with etrolizumab treatment also showed that the higher GZMA level in colonic tissue was associated with increased clinical remission and mucosal healing, suggesting that GZMA could serve as a potential therapeutic target [29]. In contrast, another work found that GZMA was upregulated in the serum and colonic tissue of DSS-induced mice, and the alleviation of intestinal inflammation was observed after knocking out GZMA in DSS-induced mice [15]. What's more, a previous study has found that the frequency of perforin or GZMA mRNA-expressing cells is increased several fold in the intestinal mucosa of patients with IBD compared with controls [30]. These studies indicated the difference in the intestinal environment between IBD patients and DSS-induced mice. Considering the intricate in vivo environment, further investigation was inquired to elucidate whether there was a feedback loop in modulation of GZMA expression mediated by ferroptosis due to the fact that the differentiation of IECs was accompanied by an increase in GPX4 protein expression. In addition, the further study was required to discuss the work that how ferroptosis regulated CDX2 expression and elucidate the other possible forms of cell death, such as including disulfidptosis, necroptosis, cuproptosis signaling pathways involved in GZMA-mediated cell differenitation, the potential roles of GZMA on IBD, such as drug resistance, gut microbiota, and intestinal fibrosis, would be explored in our next work.

Classical cAMP signaling is an essential intracellular messenger that regulates various cellular functions, including metabolism, cell proliferation, and signal transduction [31–33]. Our previous research has found that targeting PDE4 with DIP to increase cAMP levels could alleviate intestinal inflammation [13], indicating that PDE4 is an important therapeutic target for IBD. In this work, we found GZMA could suppress PDE4 phosphorylation to activate PKA/CREB cascade signaling, of note, no significant changes of AC6 activation, a member of adenylyl cyclase (ADCY) enzymes responsible for the synthesis of cyclic adenosine monophosphate (cAMP) from adenosine triphosphate (ATP), was observed in response to GZMA, which suggested the critical role of PDE4 inhibition in improvement of IBD was reported in our previous work [12, 34]. Further research would be performed to address how GZMA regulated PDE4 phosphorylation.

Conclusions

This study extended the novel role and mechanism of GZMA in improvement of intestinal epithelial integrity in IBD through inhibition of GPX4-mediated ferroptosis mediated by PDE4/PKA/CREB cascade signaling.

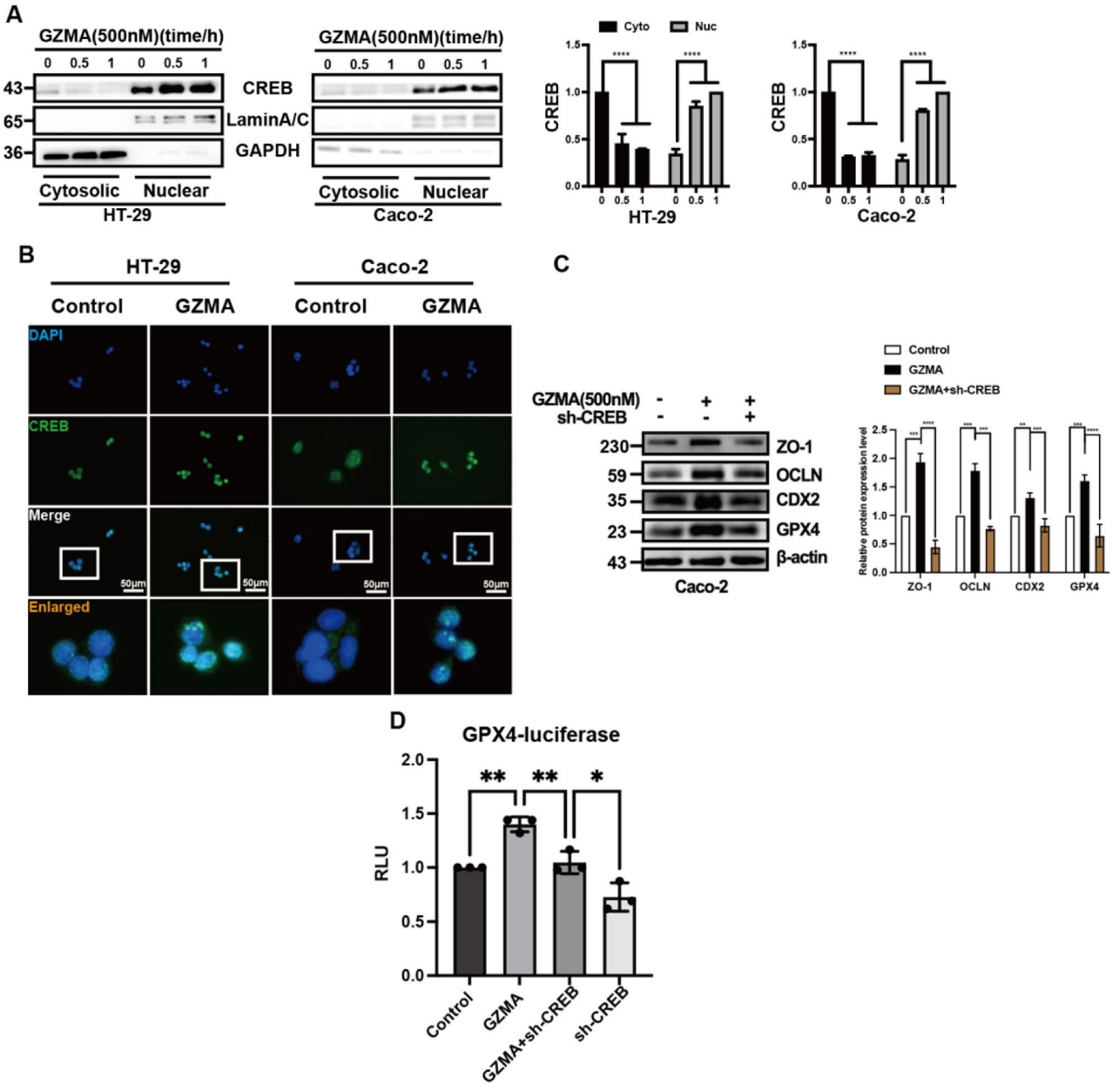

Fig. 4 GZMA modulated CREB nuclear translocation to promote intestinal epithelial integirty (**A**) HT-29 and Caco-2 cells were serum-starved for 24 h, followed by stimulation with GZMA (500 nM) for indicated time. Cell cytoplasmic and nuclear proteins were extracted to detect CREB. Data represent the mean ± s.d. of three independent experiments and were analyzed by one-way ANOVA with multiple comparisons, followed by Dunnett post hoc test for significance versus Control, ****$p < 0.0001$. the control was normalized as 1. **(B)** Immunofluorescence of CREB localization in HT-29 and Caco-2 cells treated with or without GZMA for 1 h after serum starved for 24 h. **(C)** western blotting was conducted to analyze the expression of the specific proteins in Caco-2 cells after transferd with sh-CREB plasmid, followed by stimulation with GZMA (500 nM) for 48 h. Data represent the mean ± s.d. of three independent experiments and were analyzed by one-way ANOVA with multiple comparisons, followed by Dunnett post hoc test for significance versus Control, **$p < 0.01$, ***$p < 0.001$, ****$p < 0.0001$. The control was normalized to 1. **(D)** After co-transfected with indicated plasmids combined with GPX4-Luc plasmid, sh-CREB plasmids and a control Renilla luciferase expression vector for 48 h, 293T cells were treated with or without GZMA(500 nM) for 48 h, the relative luciferase unit (RLU) was presented as the fold activation relative to Renilla luciferase activity. Data represent the mean ± s.d. of three independent experiments and were analyzed by two-way ANOVA, followed by Dunnett post hoc test for significance versus Control. *$p < 0.05$, ***$p < 0.01$

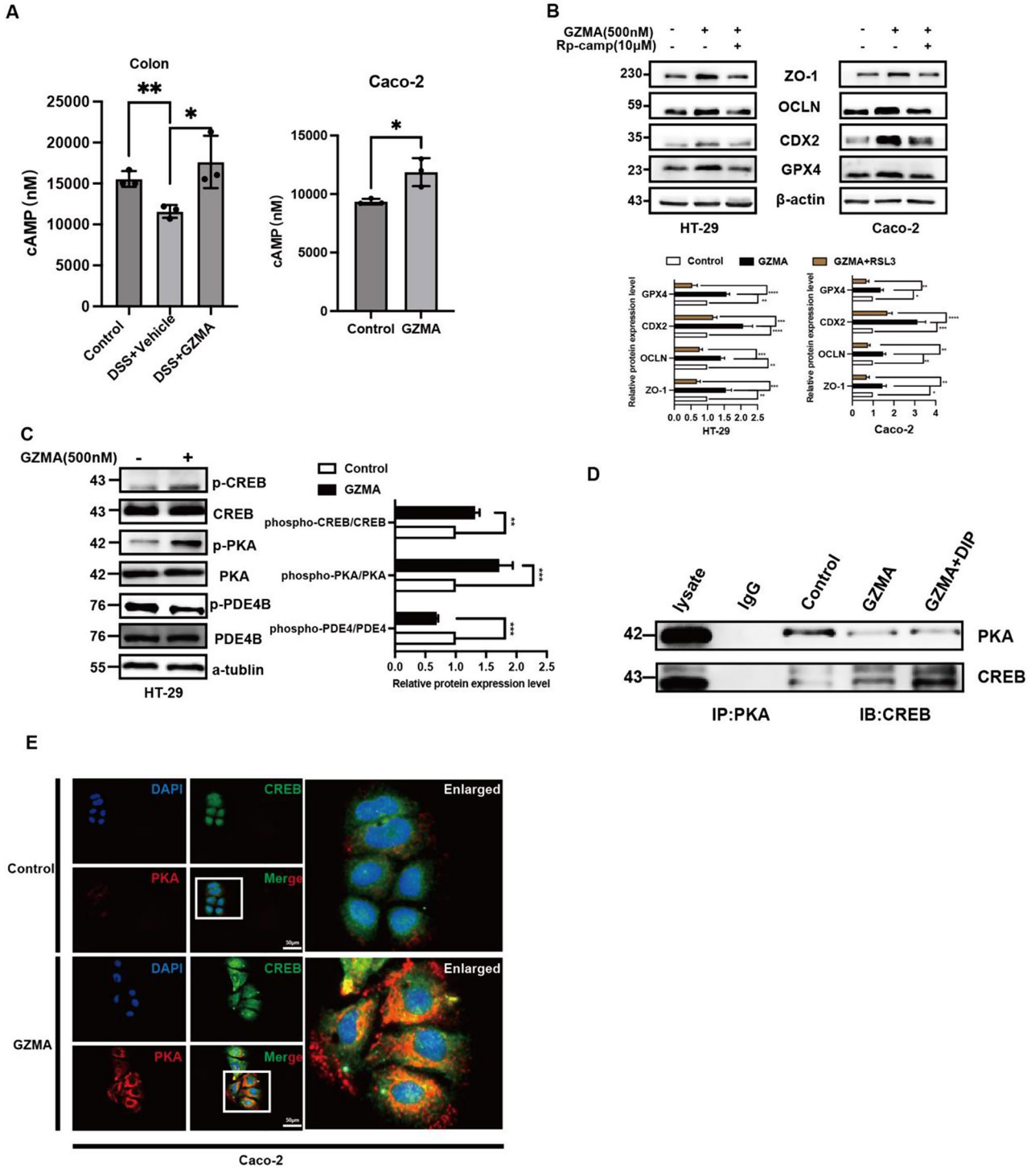

Fig. 5 GZMA modulated PDE4/PKA/CREB cascade signaling. **(A)** The level of cAMP was measured by Elisa according to the instruction. Data presented as the means ± s.d. of three independent experiments and were analyzed by one-way ANOVA (left panel) and two sample t test (right panel), $*p < 0.05$. **(B)** HT-29 and Caco-2 cells were serum-starved for 24 h, followed by stimulation with GZMA (500 nM) for 1 h followed by addition of with Rp-cAMPS (10 μM) for 48 h, WB was conducted to analyze the indicated protein. The band was quantified and analyzed by one-sample t test for significance, the control was normalized as 1, data represent the mean ± s.d. $***p < 0.001$, $**p < 0.01$, $****p < 0.0001$. **(C)** after starvation overnight, HT-29 cells were treated with GZMA for 1 h, and the total protein was collected to detect indicated protein, Data was presented as the mean ± s.d. of three independent experiments and were analyzed by one-way ANOVA (left panel) and two sample t test (right panel), $**p < 0.01$, $***p < 0.001$. **(D)** Caco-2 cells were serum starved for 24 h after 80% confluence, then stimulated as indicated for 1 h. Immunoprecipitated (IP) was employed to analyze the interaction between PKA and CREB. **(E)** Immunofluorescence of co-localization between PKA and CREB in Caco-2 cells treated with or without GZMA for 1 h after serum starved for 24 h. scale bar = 50 μm

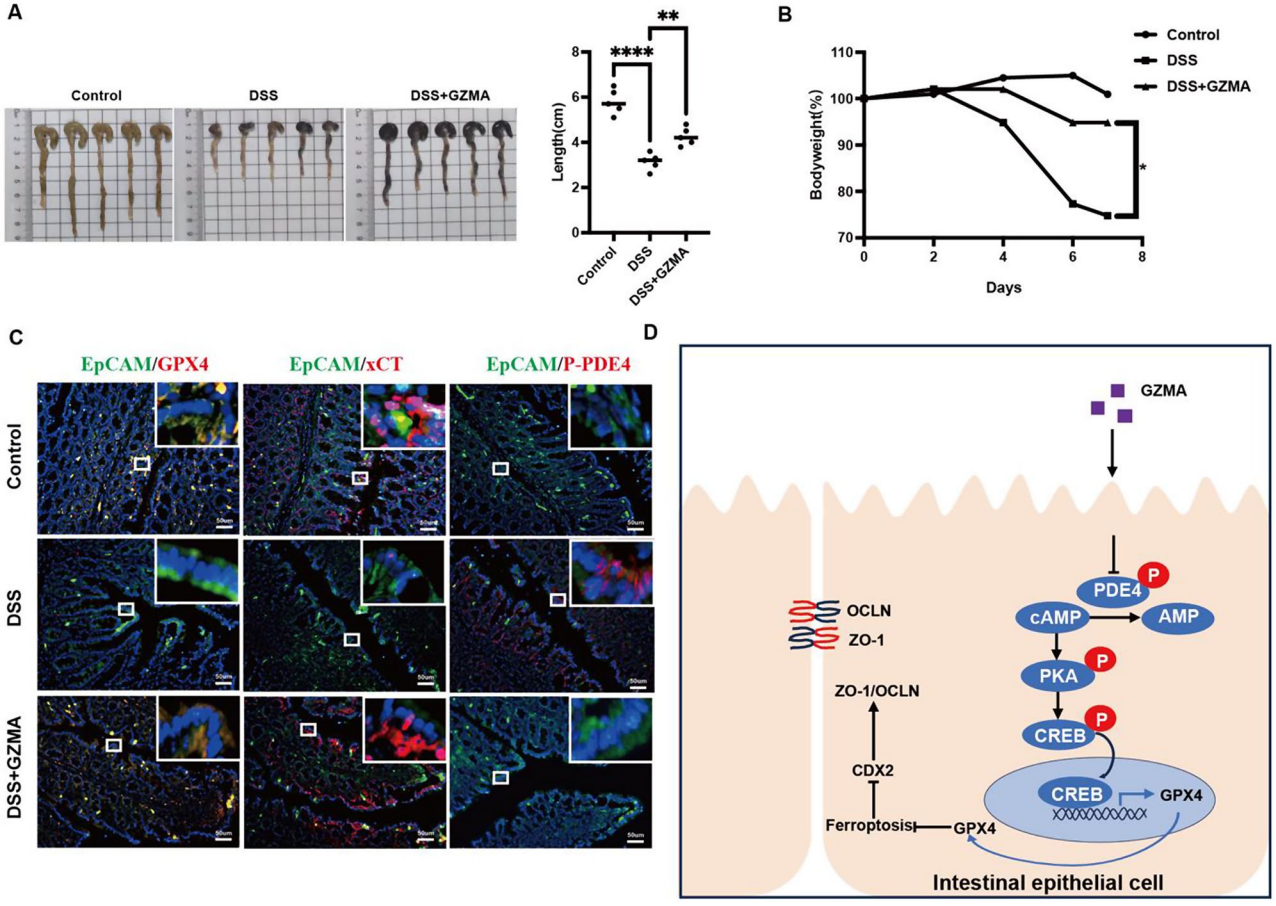

Fig. 6 GZMA improved DSS-induced colitis in vivo **(A)** Representative colon length and **(B)** body weight changes in indicated group were measured and analyzed by one way ANOVA, The body weight changes were expressed as the percentage of initial body weight at the start of the experiments as 100%, *** $p < 0.001$, ** $p < 0.01$. **(C)** Immunofluorescence was performed to detect GPX4, xCT and phosphorylation of PDE4 expression in indicated group. **(D)** Schematic model of GZMA regulating IEC differentiation through ferroptosis

Abbreviations

CD	Crohn's disease
CDX2	Caudal-related homeobox transcription factor-2
cAMP	cyclic adenosine monophosphate
CREB	cAMP-response element binding protein
CTLs	cytotoxic T lymphocytes
DMEM	Dulbecco's Modified Eagle Medium
DSS	Dextran sulfate sodium
FACS	Fluorescence Activating Cell Sorter
FBS	Fetal bovine serum
IP	Immunoprecipitation
IBD	inflammatory bowel disease
IF	immunofluorescence
IECs	intestinal epithelial cells
GZMA	Granzyme A
GPX4	Glutathione Peroxidase 4; Granzyme A
MFI	mean fluorescence intensity
NK	natural killer
OCLN	occludin
PDE4	Phosphodiesterase 4
PBS	phosphate Buffer solution
QPCR	quantitative polymerase chain reaction
ROS	reactive oxygen species
RLU	relative luciferase unit
SLC7A11	Solute carrier family 7 member 11
SDS-PAGE	sodium dodecyl sulfate polyacrylamide gel electrophoresis
UC	ulcerative colitis
WB	western blotting
ZO-1	zonula occludens-1

Supplementary Information

The online version contains supplementary material available at https://doi.org/10.1186/s12964-024-01836-y.

Supplementary Material 1: Primer sequence for real-time PCR

Supplementary Material 2: Criteria for the Histological Score

Acknowledgements
Not applicable.

Author contributions
MY, WFX, and STG conceived and designed the experiments, RWN, JLL, DXL, HC, JXW, XYZ and LX performed experiments, RWN, JLL, JXW, XYZ, ZLL, LX and LLG analyzed the data, MY, STG and WFX wrote the manuscript and revised manuscript. All authors read and approved the final revised manuscript.

Funding
This work was supported by National Natural Science Foundation of China (No.82070537, No.82200607). Guangdong Basic and Applied Basic Research Foundation (No.2020A1515110109, No.2021A1515012194, No.2023A1515030064). Accurate diagnosis, treatment and prevention

strategies for digestive system diseases related to diarrhea in children (2023YFC2706500), Guangzhou key laboratory of Pediatric Inflammatory Bowel Disease (2023A03J0866), Guangzhou Clinical Medicine Institute of Pediatric Digestive (011009003). Basic and applied research project of Guangzhou Municipal Science and Technology Project (No.202201020631).

Data availability
No datasets were generated or analysed during the current study.

Declarations

Ethical approval
Upon the declaration of Helsinki, the clinical sample experiment and all animal experiments were reviewed and approved by the Medical Ethics Committee for Clinical Ethical Review and animal committee of Guangdong Provincial People's Hospital (KY-Z-2022-164-03), respectively. The patients gave written informed consent for their clinical records used, which are not publicly available; however, it could be available upon request.

Consent for publication
All authors have agreed to publish this manuscript.

Competing interests
The authors declare no competing interests.

Received: 24 March 2024 / Accepted: 17 September 2024
Published online: 04 October 2024

References

1. Peterson LW, Artis D. Intestinal epithelial cells: regulators of barrier function and immune homeostasis. Nat Rev Immunol. 2014;14(3):141–53.
2. Zeisel MB, Dhawan P, Baumert TF. Tight junction proteins in gastrointestinal and liver disease. Gut. 2019;68(3):547–61.
3. Horowitz A, et al. Paracellular permeability and tight junction regulation in gut health and disease. Nat Rev Gastroenterol Hepatol. 2023;20(7):417–32.
4. Fanning AS, et al. The tight junction protein ZO-1 establishes a link between the transmembrane protein occludin and the actin cytoskeleton. J Biol Chem. 1998;273(45):29745–53.
5. Pan W et al. *Vitronectin Destroyed Intestinal Epithelial Cell Differentiation through Activation of PDE4-Mediated Ferroptosis in Inflammatory Bowel Disease.* Mediators of Inflammation, 2023. 2023: p. 6623329.
6. Coskun M, Troelsen JT, Nielsen OH. The role of CDX2 in intestinal homeostasis and inflammation. Biochim Biophys Acta. 2011;1812(3):283–9.
7. Crissey MAS et al. Cdx2 levels modulate intestinal epithelium maturity and paneth cell development. Gastroenterology, 2011. 140(2).
8. Takayama K, et al. Generation of human iPSC-Derived intestinal epithelial cell monolayers by CDX2 transduction. Cell Mol Gastroenterol Hepatol. 2019;8(3):513–26.
9. Wang J, et al. Moderate Treadmill Exercise modulates gut microbiota and improves intestinal barrier in High-Fat-Diet-Induced obese mice via the AMPK/CDX2 Signaling Pathway. Diabetes Metabolic Syndrome Obesity: Targets Therapy. 2022;15:209–23.
10. Xu M, et al. Ferroptosis involves in intestinal epithelial cell death in ulcerative colitis. Cell Death Dis. 2020;11(2):86.
11. Mayr L, et al. Dietary lipids fuel GPX4-restricted enteritis resembling Crohn's disease. Nat Commun. 2020;11(1):1775.
12. Pan W et al. *Vitronectin Destroyed Intestinal Epithelial Cell Differentiation through Activation of PDE4-Mediated Ferroptosis in Inflammatory Bowel Disease.* Mediators Inflamm, 2023. 2023: p. 6623329.
13. Huang B et al. Mucosal profiling of Pediatric-Onset Colitis and IBD reveals common pathogenics and therapeutic pathways. Cell, 2019. 179(5).
14. Anthony DA, et al. Functional dissection of the granzyme family: cell death and inflammation. Immunol Rev. 2010;235(1):73–92.
15. Santiago L, et al. Extracellular Granzyme A promotes colorectal Cancer Development by enhancing gut inflammation. Cell Rep. 2020;32(1):107847.
16. Martinvalet D, et al. Granzyme A cleaves a mitochondrial complex I protein to initiate caspase-independent cell death. Cell. 2008;133(4):681–92.
17. Zhou Z, et al. Granzyme A from cytotoxic lymphocytes cleaves GSDMB to trigger pyroptosis in target cells. Volume 368. New York, N.Y.): Science; 2020. 6494.
18. Zhang D, et al. Granzymes A and B directly cleave lamins and disrupt the nuclear lamina during granule-mediated cytolysis. Proc Natl Acad Sci USA. 2001;98(10):5746–51.
19. Xiong J, et al. Protein kinase D2 protects against Acute Colitis Induced by Dextran Sulfate Sodium in mice. Sci Rep. 2016;6:34079.
20. Zhang S, et al. Inhibition of CREB-mediated ZO-1 and activation of NF-κB-induced IL-6 by colonic epithelial MCT4 destroys intestinal barrier function. Cell Prolif. 2019;52(6):e12673.
21. Jia T, et al. CRISPR/Cas13d targeting GZMA in PARs pathway regulates the function of osteoclasts in chronic apical periodontitis. Cell Mol Biol Lett. 2023;28(1):70.
22. Wang T, et al. TGF-beta induced PAR-1 expression promotes tumor progression and osteoclast differentiation in giant cell tumor of bone. Int J Cancer. 2017;141(8):1630–42.
23. Panse N, Gerk PM. The Caco-2 Model: modifications and enhancements to improve efficiency and predictive performance. Int J Pharm. 2022;624:122004.
24. Briske-Anderson MJ, Finley JW, Newman SM. *The influence of culture time and passage number on the morphological and physiological development of Caco-2 cells.* Proceedings of the Society For Experimental Biology and Medicine. Society For Experimental Biology and Medicine (New York, N.Y.), 1997. 214(3): pp. 248–257.
25. Lu S, et al. Transport properties are not altered across Caco-2 cells with heightened TEER despite underlying physiological and ultrastructural changes. J Pharm Sci. 1996;85(3):270–3.
26. Wang Z et al. CREB stimulates GPX4 transcription to inhibit ferroptosis in lung adenocarcinoma. Oncol Rep, 2021. 45(6).
27. Zhang H, et al. Complex roles of cAMP-PKA-CREB signaling in cancer. Experimental Hematol Oncol. 2020;9(1):32.
28. Hadian K, Stockwell BR. The therapeutic potential of targeting regulated non-apoptotic cell death. Nat Rev Drug Discov. 2023;22(9):723–42.
29. Tew GW et al. Association between Response to Etrolizumab and expression of integrin αE and granzyme A in Colon biopsies of patients with Ulcerative Colitis. Gastroenterology, 2016. 150(2).
30. Müller S, et al. Activated CD4 + and CD8 + cytotoxic cells are present in increased numbers in the intestinal mucosa from patients with active inflammatory bowel disease. Am J Pathol. 1998;152(1):261–8.
31. Musheshe N, Schmidt M, Zaccolo M. cAMP: from Long-Range Second Messenger to Nanodomain Signalling. Trends Pharmacol Sci. 2018;39(2):209–22.
32. Zaccolo M, Zerio A, Lobo MJ. Subcellular Organization of the cAMP signaling pathway. Pharmacol Rev. 2021;73(1):278–309.
33. Arumugham VB, Baldari CT. cAMP: a multifaceted modulator of immune synapse assembly and T cell activation. J Leukoc Biol. 2017;101(6):1301–16.
34. Huang B, et al. Mucosal profiling of Pediatric-Onset Colitis and IBD reveals common pathogenics and therapeutic pathways. Cell. 2019;179(5):1160–e117624.

Publisher's note